Journal of Chromatography A, 1218 (2011) 4322–4331

Contents lists available at ScienceDirect

Journal of Chromatography A

journal homepage: www.elsevier.com/locate/chroma

# Monolithic capillary columns synthesized from a single phosphate-containing dimethacrylate monomer for cation-exchange chromatography of peptides and proteins

Xin Chen [a], H. Dennis Tolley [b], Milton L. Lee [a,*]

[a] Department of Chemistry and Biochemistry, Brigham Young University, Provo, UT 84602, USA
[b] Department of Statistics, Brigham Young University, Provo, UT 84602, USA

ARTICLE INFO

*Article history:*
Received 26 October 2010
Received in revised form 22 February 2011
Accepted 24 April 2011
Available online 6 May 2011

*Keywords:*
Liquid chromatography
Capillary columns
Cation exchange
Monolithic stationary phase
Phosphate group
Proteins/peptides

ABSTRACT

Monoliths containing phosphoric acid functional groups were synthesized from only one monomer, bis[2-(methacryloyloxy)ethyl] phosphate (BMEP), in 75-μm i.d. UV transparent fused-silica capillaries by photo-initiated polymerization for cation exchange chromatography of peptides and proteins. Various synthetic conditions, including porogen solvents, monomer concentration, and polymerization time, were studied. The hydrophobicities of the resulting monoliths were evaluated using propyl paraben under reversed-phase conditions and synthetic peptides under ion-exchange conditions. These monoliths exhibited low hydrophobicities and relatively low porosities due to their highly cross-linked structures. A dynamic binding capacity (lysozyme) of 73 mg/mL of column volume was measured using the best performing monolith. Synthetic peptides were eluted in approximately 30 min without addition of acetonitrile to the mobile phase, yielding a peak capacity of 28. Efficiencies of 52,900 plates/m for peptides and 71,000 plates/m for proteins were obtained under isocratic conditions. The effects of separation conditions, i.e., mobile phase pH and salt gradient rate, were studied. Good run-to-run reproducibility was achieved with a relative standard deviation (RSD) less than 1.5% for retention times of proteins. The column-to-column retention time reproducibility for peptides was less than 3.5% RSD. A monolithic column was used to follow the deamidation of ribonuclease A. The kinetics of deamidation were founded to be first order with a half life of 195 h. A cytochrome C digest was also separated using a linear gradient of sodium chloride.



## 1. Introduction

Ion-exchange chromatography (IEC) is an important chromatographic separation mode for analytes that can participate in ionic interactions, such as peptides, proteins, oligonucleotides, and viruses [1–4]. Compared to other chromatographic separation modes, such as reversed-phase chromatography (RPC) and affinity chromatography, IEC employs mild separation conditions that avoid denaturing of the proteins. IEC is often used in two-dimensional separations for peptide mapping of protein digests [5,6], where it is followed by RPC, which is an orthogonal separation mechanism.

Monoliths are considered to be emerging chromatographic stationary phases, which provide an alternative to particle packed columns. They provide lower back pressure in liquid chromatography (LC) and are easy to prepare. Several reviews have described the synthetic methods and applications of monoliths in LC [7–14]. Polymeric monolithic columns are typically used to separate biomolecules due to their pH stability and biocompatibility. Several approaches, including adsorption of surfactants [15,16], post-modification [17–20], and copolymerization [21–25], have been utilized to introduce functional groups into monolith backbones to prepare capillary cation-exchange columns. Among these approaches, copolymerization is the simplest, since it only requires one step, which leads to easy control of the total concentration of functional groups in the monolith. However, monoliths synthesized according to this approach suffer from low density of functional groups on the surface. Most of the functional groups are buried in the body of the monolith. Fortunately, the porogen solvents can be carefully optimized to produce more functional groups on the surface, thereby increasing the dynamic binding capacity (DBC) of the monolith [23–25].

Recently, several ion-exchange monoliths were prepared by various methods. Krenkova et al. [26] grafted 2-acrylamido-2-methyl-1-propanesulfonic acid and acrylic acid on a poly(2,3-dihydroxypropyl methacrylate-co-ethylene methacrylate) mono-

* Corresponding author. Tel.: +1 801 422 2135; fax: +1 801 422 0157.
*E-mail address:* milton_lee@byu.edu (M.L. Lee).

0021-9673/$ – see front matter © 2011 Elsevier B.V. All rights reserved.
doi:10.1016/j.chroma.2011.04.074

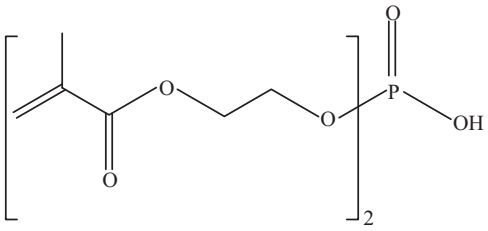


BMEP

**Fig. 1.** Chemical structure of BMEP.

lith to prepare strong and weak cation-exchange monoliths for separation of peptides and proteins. Good separations were obtained. DBC values of 29 and 21 mg/mL for strong and weak cation-exchange monoliths were measured. However, no peak capacities were reported for separations of peptides and proteins. Past work in our laboratory has been based on *in situ* copolymerization to prepare several cation-exchange monolithic columns [23,25,27]. Excellent separations of peptides and proteins were achieved in 15 min with peak capacities over 25.

Normally, a monomer and a cross-linker are the major components used to prepare a monolith. In this work, only a cross-linker was used to prepare a cation-exchange polymeric monolith. With only one monomer, the reproducibility of synthesized monoliths should improve, and the resulting highly cross-linked structure should ensure long-term stability. However, only a few studies of monoliths synthesized from one monomer have been reported. Lubbad and Buchmeiser [28] used tetrakis(4-vinylbenzyl)silane (TVBS) to prepare a highly cross-linked polymer to separate both low, medium and high-molecular-weight analytes. The monolith showed low swelling propensity due to the highly cross-linked structure. Greiderer et al. [29] used 1,2-bis(p-vinylphenyl)ethane (BVPE) to obtain a monolith for simultaneous separation of low and high-molecular-weight compounds. The resulting monolith showed a broad bimodal pore size distribution from flow-through channels in the μm range, and mesopores to small macropores in the range of 4–500 nm. Tremendous enhancement of surface area (101 $m^2$/g) was obtained compared to typical organic monoliths (20 $m^2$/g). Good reproducibility and low swelling propensity were also achieved due to highly cross-linked structures. Recently, a series of monoliths prepared for hydrophobic interaction chromatography was reported by our group using either polyethylene glycol diacrylate or dimethacrylate as single monomer [30]. Excellent separations of proteins with good peak capacities were obtained. The limited number of reports on monoliths synthesized from one monomer primarily results from the limited availability of suitable monomers.

In this work, bis[2-(methacryloyloxy)ethyl] phosphate (BMEP) (chemical structure shown in Fig. 1) was used as a single monomer to prepare polymeric cation exchange monolithic columns for LC by *in situ* photo-initiated copolymerization. The performance of these columns for separation of peptides and proteins under both isocratic and gradient ion-exchange conditions are presented.

## 2. Experimental

### 2.1. Materials and chemicals

Uracil, 2,2-dimethoxy-2-phenylacetophenone (DMPA, 99%), 3-(trimethoxysilyl)propyl methacrylate (TPM, 98%), BMEP, a natural peptide mixture (H2016), peptides (i.e., D-Leu-Gly, Gly-Gly-Tyr-Arg, Gly-Tyr, angiotensin II, and leucine enkephalin), proteins (i.e., trypsinogen from bovine pancrease, ribonuclease A from bovine pancrease, cytochrome C from bovine heart, α-chymotrypsinogen A from bovine pancreas, trypsin from bovine pancreas, and lysozyme from chicken egg white) were purchased from Sigma–Aldrich (Milwaukee, WI) and used without further purification. Propyl paraben was purchased from Spectrum (Gardena, CA). A synthetic peptide standard (CES-P0050) was obtained from Alberta Peptides Institute (Edmonton, Alberta, Canada). Solvents for monolith synthesis and chemicals for mobile phase preparation were HPLC or analytical reagent grade. Fused-silica capillaries (75-μm i.d. × 360-μm o.d.) were purchased from Polymicro Technologies (Phoenix, AZ, USA).

### 2.2. Preparation of polymeric monolithic columns

UV-transparent fused-silica capillaries were first silanized with TPM to introduce pendant vinyl groups to anchor the polymer monolith to the capillary wall [24,31]. Polymeric monoliths were prepared as previously described [23]. The polymerization mixture was prepared in a 4 mL glass vial by mixing initiator, monomers, and porogens. The mixture was vortexed and ultrasonicated for 1 min to help form a homogeneous solution and eliminate oxygen. The monomer solution was introduced into the capillary by capillary action. The capillary was placed directly under a PRX 1000-20 Exposure Unit UV lamp (TAMARACK Scientific, Corona, CA) for various times (2–10 min). The resulting monolith was then flushed with methanol and water sequentially for 30 min each to remove porogens and unreacted monomers using an LC pump. The capillaries were stored in 10% methanol aqueous solutions to prevent the monoliths from drying. Scanning electron microscopy (SEM) images of the monoliths were obtained as previously described [23].

### 2.3. Capillary LC

Capillary LC of peptides and proteins was performed using an LC system comprised of two ISCO 100 DM syringe pumps and a flow controller. A Valco splitting tee (Houston, TX) was positioned between the static mixer of the syringe pumps and the 60-nL Valco internal loop sample injector. A 40-cm-long capillary (30-μm i.d.) was used as a capillary splitter and a 10-cm-long capillary (30-μm i.d.) was connected between the splitting tee and the injector. The mobile phase flow rate was set at 40 μL/min, and the actual flow rate in the monolithic capillary column was approximately 0.32 μL/min. The mobile phase was 5 mmol/L aqueous phosphate buffer at various pH values. All mobile phases were filtered through a 0.2 μm Nylon membrane filter (Supelco, Bellefonte, PA). A Model UV3000 detector from Thermo Separations (San Jose, CA) was used at a wavelength of 214 nm. Data were acquired with ChromQuest 2.5.1 software (ThermoQuest, San Jose, CA). Capillary LC of a cytochrome C digest was performed using an Ultimate 3000 high pressure gradient LC system (Dionex, Sunnyvale, CA) equipped with an FLM-3300 nano flow manager [30]. A section of 50 μm i.d. poly(vinyl alcohol)-coated fused silica capillary was used as the sample loop, and the loop volume was calculated to be 200 nL. Detailed chromatographic conditions are given in the figure captions.

For evaluation of the relative hydrophobicities of the monoliths, reversed-phase capillary LC elution measurements of propyl paraben and uracil were performed. The mobile phase was 20% (v/v) acetonitrile in water. The pump flow rate was 40 μL/min, and the detection wavelength was 254 nm. Uracil was used as an unretained marker. The retention factor for propyl paraben was obtained from the equation, $k = (t_p - t_u)/t_u$, where $k$ is the retention factor, and $t_p$ and $t_u$ are the retention times of propyl paraben and uracil, respectively.

**Table 1**
Compositions and physical properties of monoliths.

| Column | BMEP (g) | Methanol (g) | Dodecanol (g) | DMPA (g) | UV exposure time (min) | Porosity (%) | Hydrophobicity |
|---|---|---|---|---|---|---|---|
| 1 | 0.60 | 1.15 | 0.35 | 0.006 | 3 | 64 | 0.489 |
| 2 | 0.60 | 1.18 | 0.32 | 0.006 | 3 | 62 | 0.451 |
| 3 | 0.60 | 1.20 | 0.30 | 0.006 | 3 | 57 | 0.454 |
| 4 | 0.55 | 1.18 | 0.32 | 0.006 | 3 | 64 | 0.484 |
| 5 | 0.58 | 1.18 | 0.32 | 0.006 | 3 | 63 | 0.420 |
| 6 | 0.65 | 1.18 | 0.32 | 0.006 | 3 | 55 | 0.439 |
| 7 | 0.60 | 1.18 | 0.32 | 0.006 | 2 | 68 | 0.447 |
| 8 | 0.60 | 1.18 | 0.32 | 0.006 | 5 | 61 | 0.479 |
| 9 | 0.60 | 1.18 | 0.32 | 0.006 | 10 | 58 | 0.488 |

### 2.4. DBC measurements

The DBC was examined via frontal analysis following a procedure described previously [23]. The column was first equilibrated with 5 mmol/L sodium phosphate buffer at pH 6.0, and then a solution of 3.15 mg/mL lysozyme in buffer was pumped through the column at a pump flow rate of 40 μL/min. The mobile phase flow rate in the monolithic capillary column was measured using a calibration capillary (Eksigent, Livermore, CA). The binding capacity was calculated at 50% of the final absorbance value of the breakthrough curve and expressed in mg/mL of column volume.

### 2.5. Separation of protein digest

A cytochrome C digest was prepared according to a published procedure [26]. Cytochrome C (3.20 mg/mL) was diluted with 100 mmol/L ammonium bicarbonate solution. Trypsin was added at a substrate-to-enzyme ratio of 50:1 (w/w) and the solution was incubated at 37 °C for 20 h. Proteolysis was terminated by decreasing the pH below 2 by adding formic acid to the solution. The digest was then desalted using a Sep-Pak Vac 3cc C18 Cartridge (Waters, Milford, MA) following the protocol suggested by the manufacturer. The peptide solutions in the microvials were vacuum-dried to pellets that were redissolved in 300 μL 5 mmol/L sodium phosphate buffer at pH 3.0 for separation.

### 2.6. Separation of deamidation variants of ribonuclease A

The deamidation variants of ribonuclease A were prepared according to a protocol provided by Dionex [32]. A 334 μL volume of 15 mg/mL ribonuclease A, 100 μL 10% (wt %) ammonium bicarbonate, and 566 μL water were combined in a microvial and incubated at 37 °C. Then, 50 μL aliquots were withdrawn periodically and frozen for future analysis.

## 3. Results and discussion

### 3.1. Monolith prepared from a single monomer

BMEP, which is a commercial cross-linker, was chosen as a monomer to prepare a cation-exchange monolith because it contains the desirable phosphate functional group. This cross-linker was previously used to synthesize cation-exchange monolithic columns with a second monomer, polyethylene glycol acrylate (PEGA) [27]. The BMEP–PEGA monoliths demonstrated excellent separation of peptides and proteins in the cation-exchange mode. However, PEGA is no longer commercially available, probably due to the reactivity of the acrylate group. Since BMEP has two reactive methacrylate end groups, it can be used as a single monomer to synthesize a cation-exchange monolith.

Methanol, dodecanol, and ethyl ether were evaluated as porogen solvents in previous work to synthesize BMEP-PEGA monoliths. We initially evaluated combinations of the same three solvents for the synthesis of BMEP-only monoliths. However, the resulting monolith morphologies were not uniform when observed under the microscope, even after trying various ratios of the solvents. With methanol and ethyl ether as porogen solvents, the monoliths demonstrated low efficiencies (lower than 2000 plates/m) for separations of peptide and protein standards. Methanol and dodecanol were finally selected as the preferred porogen solvents, since the morphologies of the monoliths appeared uniform under the microscope. Several monoliths were prepared as listed in Table 1. These monolithic columns exhibited low hydrophobicities compared to monoliths prepared previously [23–25] (see Table 1).

### 3.2. Effect of porogen solvents on the separation of peptides and proteins

Selection of the porogen solvent(s) has a great effect on the morphology of the resulting monolith, thus, affecting significantly the separation. Methanol is a “good” solvent, which leads to late phase separation during polymerization and results in small pores [33]. With more methanol in the porogens, the back pressure of the monolith increases, while the total porosity decreases (columns 1–3 in Table 1). These three columns were used to separate peptide and protein standards. CES P0050 is a mixture of four undecapeptides designed for evaluation of particle packed strong cation-exchange columns [23,34]: Ac-Gly-Gly-Gly-Leu-Gly-Gly-Ala-Gly-Gly-Leu-Lys-amide, Ac-Lys-Tyr-Gly-Leu-Gly-Gly-Ala-Gly-Gly-Leu-Lys-amide, Ac-Gly-Gly-Ala-Leu-Lys-Ala-Leu-Lys-Gly-Leu-Lys-amide, and Ac-Lys-Tyr-Ala-Leu-Lys-Ala-Leu-Lys-Gly-Leu-Lys-amide. The protein standard mixture contained five proteins including trypsinogen, ribonuclease A, cytochrome C, α-chymotrypsinogen A, and lysozyme. Longer times were required to elute peptides and proteins from monoliths prepared with more methanol in the porogens (Table 2). Peak capacities (time of gradient/peak width) of 16 and 15 were obtained for peptides and proteins using column 2 (10.5 cm × 75 μm). These peak capacities are greater than those obtained using column 3 and similar to column 1. However, the peak shapes of peptides and proteins were better with column 2 than those with column 1 (chromatography not shown).

### 3.3. Effect of BMEP percentage in the reaction mixture on the separation of peptides and proteins

Considering the trade-off between retention time and resolution, the porogen system of column 2 was selected for further experiments. The monomer percentage in the reaction mixture alters both the monolith morphology and the monolith composition. With a higher percentage of monomer in the preparation of the monolith, the back pressure of the monolith increased and the porosity decreased (columns 2 and 4–6 in Table 1). When the BMEP percentage in the solution was lower than 26.8% (w/w) (column 4, 10.5 cm × 75 μm), the monolith was not rigid. When it was higher than 31.8% (w/w), the mobile phase could not flow through the

**Table 2**
Effect of porogen solvents on the separation of peptides and proteins.[a]

| Column | Length (cm) | Peptides | | | | | | | | Proteins | | | | | | | | $R_s$[d] | Peak capacity[e] |
|---|---|---|---|---|---|---|---|---|---|---|---|---|---|---|---|---|---|---|---|
| | | Peak 1 | | Peak 2 | | Peak 3 | | Peak 4 | | Peak 1 | | Peak 2 | | Peak 3 | | Peak 4 | | Peak 5 | | | |
| | | $t_R$[b] | $w_d$[c] | $t_R$ | $w_d$ | $t_R$ | $w_d$ | $t_R$ | $w_d$ | $t_R$ | $w_d$ | $t_R$ | $w_d$ | $t_R$ | $w_d$ | $t_R$ | $w_d$ | $t_R$ | $w_d$ | | |
| 1 | 10.5 | 0.958 | 0.50 | 7.09 | 0.51 | 8.95 | 0.52 | 13.9 | 0.83 | 5.89 | 0.36 | 7.05 | 0.39 | 8.26 | 0.49 | 9.26 | 0.66 | 12.0 | 0.95 | 3.56 | 17 |
| 2 | 10.5 | 2.68 | 0.68 | 13.5 | 0.44 | 16.2 | 0.44 | 26.4 | 0.95 | 9.57 | 0.53 | 11.7 | 0.50 | 13.6 | 0.57 | 15.4 | 0.71 | 20.8 | 1.10 | 3.55 | 16 |
| 3 | 10.5 | 6.13 | 1.20 | 26.3 | 1.22 | 37.3 | 0.77 | 79.0 | 2.80 | 22.8 | 1.16 | 29.6 | 1.05 | 30.8 | 0.63 | 33.7 | 1.46 | 38.6 | 1.84 | 1.43 | 7 |

[a] *Conditions*: 100% A to 100% B in 10 min, followed by 100% B, where A was 5 mmol/L phosphate buffer at pH 3.0 for peptides and 6.0 for proteins, and B was 1 mol/L NaCl in A, 40 μL/min pump flow rate, on column detection at 214 nm.
[b] $t_R$ is retention time in min.
[c] $w_d$ is peak width in min.
[d] Resolution between protein peaks 2 and 3.
[e] Peak capacity was calculated from gradient time/peak width for peptides. Peptides 1–4 represent Ac-Gly-Gly-Gly-Leu-Gly-Gly-Ala-Gly-Gly-Leu-Lys-amide, Ac-Lys-Tyr-Gly-Leu-Gly-Gly-Ala-Gly-Gly-Leu-Lys-amide, Ac-Gly-Gly-Ala-Leu-Lys-Ala-Leu-Lys-Gly-Leu-Lys-amide, and Ac-Lys-Tyr-Ala-Leu-Lys-Ala-Leu-Lys-Gly-Leu-Lys-amide, respectively. Proteins 1–5 represent trypsinogen, α-chymotrypsinogen A, cytochrome C, ribonuclease A, and lysozyme, respectively.




**Fig. 2.** Breakthrough curves for lysozyme on monoliths polymerized for various times. Conditions: 8.1, 9.2, 9.2, and 7.0 cm × 75 μm i.d. for columns 2 (C), 7 (A), 8 (B), and 9 (D), respectively; 5 mmol/L phosphate at pH 6.0 mobile phase; 3.15 mg/mL lysozyme in the mobile phase; 40 μL/min pump flow rate; online UV detection at 214 nm.

monolith at a pressure of 3000 psi. With an increase in percentage of BMEP in the monolith reaction mixture, the elution times for both peptides and proteins increased. It is reasonable to conclude that higher percentage of BMEP leads to larger surface area as reported previously [28–30], and more phosphate groups are exposed on the surface of the monolith. When 30.2% (w/w) BMEP was used (monolith 6, 10.5 cm × 75 μm), it took approximately 100 min for the last peptide to elute. The resolution of peptides and proteins also increased with an increase in concentration of BMEP in the monolith. Good peak profiles were obtained using these monoliths for both peptides and proteins. For the separation of CES P0050, peak capacities of 28, 23, and 16 were obtained using columns 4, 5, and 2, respectively, and peak capacities of 25, 20, and 15 were obtained for separation of proteins. Although peak capacities are higher for columns 4 and 5, peak resolution, especially the resolution between cytochrome C and ribonuclease A, was lower than with column 2 (Table 3). Considering retention time, resolution, and peak capacity, the conditions for column 2 were selected for further studies.

### *3.4. Effect of UV exposure time on the separation of peptides and proteins*

The polymerization time affects the DBC values, properties and morphologies of the resulting monoliths. From Table 1, porosity decreased with an increase in polymerization time. To evaluate the dependence of BMEP conversion on polymerization time, DBC was measured for columns 2, 7, 8, and 9. Using frontal analysis, the DBC was measured as reported previously [23]. Since the columns were designed for ion exchange chromatography of large biomolecules, a 3.15 mg/mL lysozyme solution was used to measure the DBC of the columns. DBC values of 53.5, 51.1, 54.7, and 72.7 mg/mL of column volume were measured for columns 2, 7, 8, and 9, respectively (Fig. 2). These DBC values are approximately equal to, or higher than, various synthesized and commercial columns [26,31,35]. The sharp frontal analysis curves indicated rapid adsorption of lysozyme on these monoliths. Only one plateau was observed in the frontal analysis curves, indicating a strong cation-exchange mechanism. Obviously, an increase in the polymerization time from 2 min to 5 min had no significant effect on the conversion of BMEP on the surface of the monolith. With a further increase to 10 min, the conversion increased, as indicated by the approximately 33% increase in DBC value. Fig. 3 shows SEM images of columns 2, 7,

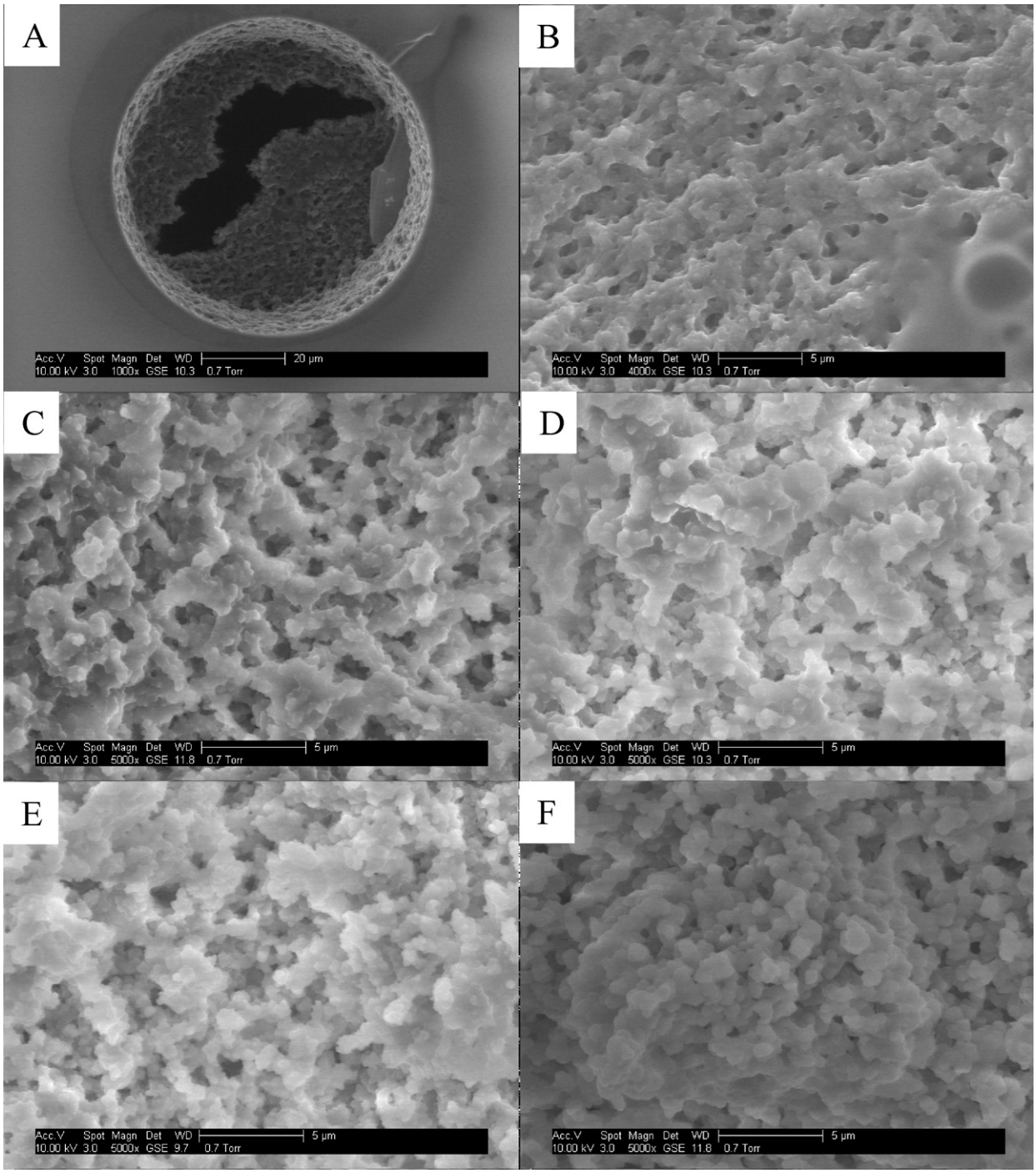


**Fig. 3.** Scanning electron micrographs of (A) column 7 (scale bar, 20 μm), (B) column 7 (scale bar, 5 μm), (C) column 2 (scale bar, 5 μm), (D) column 8 (scale bar, 5 μm), (E) column 9 (scale bar, 5 μm), and (F) column 1 (scale bar, 5 μm).

8, and 9. As can be easily seen, the morphologies are different. However, the back pressures of these monolithic columns varied only slightly. It was reported previously that the polymerization time did not affect the pore-size-distribution of monoliths significantly [36]. A similar pore-size-distribution led to a similar back pressure. The increased polymerization time also increased the rigidity of the resulting monolith. The monolith prepared with 2 min polymerization time was separated under vacuum during SEM (Fig. 3A); the other monoliths were stable under the same conditions. Although the monolith in column 7 separated, there were no gaps observed between the monolith and the column inner wall, which indicates that the monolith was covalently bonded to the capillary.

Monolithic columns 2, 7, 8, and 9 were used to separate peptides and proteins (Fig. 4). As shown, the elution times increased slightly using monoliths synthesized with longer polymerization times, except for monolithic column 9. The longer elution time for column 2 compared to column 8 was due to the longer length of column 2. The longer elution times for peptides and proteins on column 9 resulted from higher dynamic binding capacity and lower porosity. The peak capacities for peptides and proteins on columns 2, 7, 8, and 9 were 20, 16, 15, and 11, and 14, 15, 19, and

**Table 3**
Effect of BMEP concentration on the separation of peptides and proteins.[a]

| Column | Length (cm) | Peptides | | | | | | | | Proteins | | | | | | | | $R_s$[d] | Peak capacity[e] |
|---|---|---|---|---|---|---|---|---|---|---|---|---|---|---|---|---|---|---|---|
| | | Peak 1 | | Peak 2 | | Peak 3 | | Peak 4 | | Peak 1 | | Peak 2 | | Peak 3 | | Peak 4 | | Peak 5 | | | |
| | | $t_R$[b] | $w_d$[c] | $t_R$ | $w_d$ | $t_R$ | $w_d$ | $t_R$ | $w_d$ | $t_R$ | $w_d$ | $t_R$ | $w_d$ | $t_R$ | $w_d$ | $t_R$ | $w_d$ | $t_R$ | $w_d$ | | |
| 2 | 10.5 | 2.68 | 0.68 | 13.5 | 0.44 | 16.2 | 0.44 | 26.4 | 0.95 | 9.57 | 0.53 | 11.7 | 0.50 | 13.6 | 0.57 | 15.4 | 0.71 | 20.8 | 1.10 | 2.82 | 16 |
| 4 | 10.0 | 1.07 | 0.52 | 5.80 | 0.56 | 6.85 | 0.52 | 9.91 | 0.49 | 5.05 | 0.18 | 5.62 | 0.22 | 7.25 | 0.38 | 7.69 | 0.30 | 9.99 | 0.72 | 1.29 | 25 |
| 5 | 10.0 | 3.40 | 0.48 | 9.04 | 0.40 | 10.5 | 0.48 | 5.05 | 0.56 | 6.96 | 0.45 | 8.07 | 0.41 | 10.3 | 0.50 | 10.9 | 0.43 | 14.9 | 1.04 | 1.29 | 20 |
| 6 | 10.0 | 6.86 | 1.22 | 28.7 | 1.67 | 42.4 | 1.29 | 97.1 | 3.59 | 21.2 | 1.85 | 35.8 | 0.96 | 38.2 | 0.74 | 42.5 | 0.99 | 48.9 | 1.32 | 4.97 | 5 |

[a] *Conditions*: 100% A to 100% B in 10 min, followed by 100% B, where A was 5 mmol/L phosphate buffer at pH 3.0 for peptides and 6.0 for proteins, and B was 1 mol/L NaCl in A, 40 μL/min pump flow rate, on column detection at 214 nm.
[b] $t_R$ is retention time in min.
[c] $w_d$ is peak width in min.
[d] Resolution between protein peaks 3 and 4.
[e] Peak capacity was calculated from gradient time/peak width for peptides. Peptides 1–4 represent Ac-Gly-Gly-Gly-Leu-Gly-Gly-Ala-Gly-Gly-Leu-Lys-amide, Ac-Lys-Tyr-Gly-Leu-Gly-Gly-Ala-Gly-Gly-Leu-Lys-amide, Ac-Gly-Gly-Ala-Leu-Lys-Ala-Leu-Lys-Gly-Leu-Lys-amide, and Ac-Lys-Tyr-Ala-Leu-Lys-Ala-Leu-Lys-Gly-Leu-Lys-amide, respectively. Proteins 1–5 represent trypsinogen, α-chymotrypsinogen A, cytochrome C, ribonuclease A, and lysozyme, respectively.




**Fig. 4.** Effect of polymerization time on the separation of peptides and proteins. Conditions: 10.0, 10.5, 10.0, and 10.0 cm × 75 μm i.d. for columns 2, 7, 8, and 9, respectively; buffer A was 5 mmol/L phosphate at pH 6.0, buffer B was 1 M NaCl in buffer A; 2-min isocratic elution of buffer A, followed by linear gradient from buffer A to buffer B in 10 min; 40 μL/min pump flow rate; online UV detection at 214 nm. Peak identifications: (A): (1) Ac-Gly-Gly-Gly-Leu-Gly-Gly-Ala-Gly-Gly-Leu-Lys-amide, (2) Ac-Lys-Tyr-Gly-Leu-Gly-Gly-Ala-Gly-Gly-Leu-Lys-amide, (3) Ac-Gly-Gly-Ala-Leu-Lys-Ala-Leu-Lys-Gly-Leu-Lys-amide, (4) Ac-Lys-Tyr-Ala-Leu-Lys-Ala-Leu-Lys-Gly-Leu-Lys-amide; (B): (1) trypsinogen, (2) α-chymotrypsinogen A, (3) cytochrome C, (4) ribonuclease A, and (5) lysozyme.

13, respectively. Since column 8 exhibited the highest peak capacity for proteins, it was selected for additional testing.

### 3.5. Hydrophobic interactions

Hydrophobic interactions between analytes and the column are detrimental for ion exchange chromatography. Analyte retention when using a high concentration of salt in the mobile phase is strongly affected by hydrophobic interactions. A pure ion exchange mechanism can be achieved only when hydrophobic interactions are suppressed. The possible effect of hydrophobic interactions on retention times of proteins was evaluated using monolithic column 8 under isocratic conditions. The mobile phase was 5 mmol/L sodium phosphate buffer at pH 6.0 con-

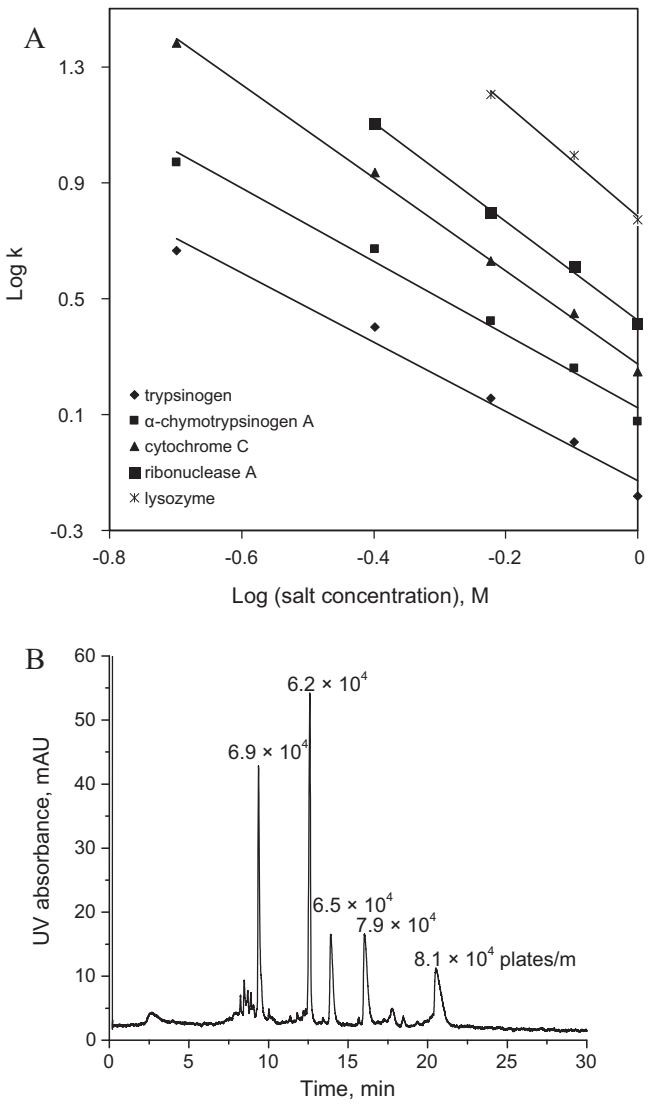


**Fig. 5.** (A) Relationship between retention factor ($K$) and salt concentration and (B) representative chromatogram (0.8 M NaCl concentration) for isocratic separation of proteins. Conditions: 8.0 cm × 75 μm i.d. column 8; buffer was 5 mmol/L phosphate with various salt concentrations at pH 6.0; 40 μL/min pump flow rate; online UV detection at 214 nm. Numbers in B represent the separation efficiency in plates/m. Peaks according to the elution order are trypsinogen, α-chymotrypsinogen A, cytochrome C, ribonuclease A, and lysozyme.

taining various concentrations of sodium chloride. As shown in Fig. 5A, a linear dependence between logarithm of retention factor and logarithm of salt concentration in the mobile phase indicates that the separation was governed by a pure ion exchange mechanism [37]. The column exhibited high efficiency for the separation of proteins without undesirable hydrophobic interactions. For example, an efficiency of approximately 71,000 plates/m was achieved for separation of proteins when 0.8 M NaCl in 5 mmol/L sodium phosphate at pH 6.0 was used as mobile phase (Fig. 5B).

The effects of acetonitrile (ACN) in the mobile phase on the retention times of peptides (CES P0050) and on peak capacity were also used to evaluate hydrophobic interactions. The retention times of peptides varied slightly with 0, 10, and 20% (v/v) ACN in the mobile phase. The peak capacity also varied only slightly. Similar retention times and constant peak capacity indicate that there are negligible hydrophobic interactions between peptides and the monolith, which confirms the low hydrophobicity of

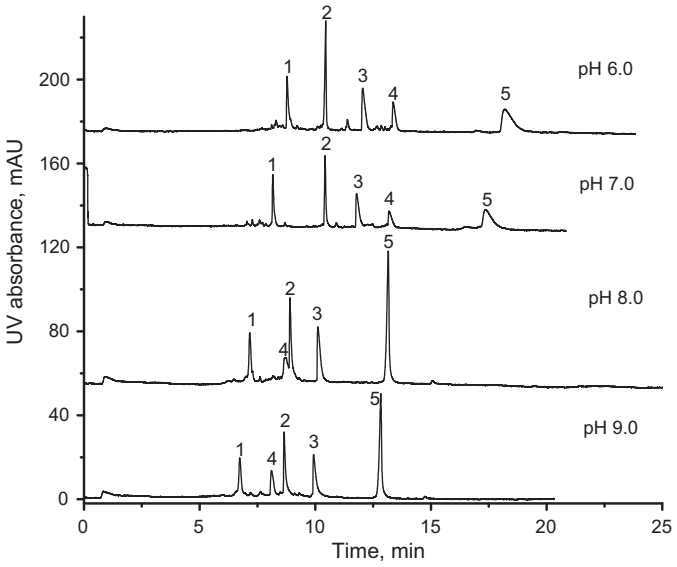


**Fig. 6.** Effect of mobile phase pH on the separation of proteins. Conditions: 10.5 cm × 75 μm i.d. column 8; buffer A was 5 mmol/L phosphate at pH 6.0, 7.0, 8.0, and 9.0, buffer B was 1 M NaCl in buffer A; 2-min isocratic elution of 100% buffer A, followed by linear gradient from 100% buffer A to 100% buffer B in 10 min; 40 μL/min pump flow rate; online UV detection at 214 nm. Peak identifications are the same as in Fig. 4B.

the monolith. A good efficiency of approximately 52,900 plates/m for the separation of peptides was obtained when 1 M NaCl in 5 mmol/L sodium phosphate at pH 3.0 was used as the mobile phase.

### 3.6. Effect of pH on monolith performance and stability

The pH of the mobile phase has an important effect on the separation of peptides and proteins in the ion-exchange mode by controlling the extent of ionization of the ion-exchange functional groups and the analytes. Since phosphoric acid is a moderately strong acid, pH values above 3.0 have a negligible effect on its ionization. The synthetic peptides in CES P0050 are all undecapeptides that have no acidic residues. Therefore, they have the same charges in acidic to neutral buffers. In theory, pH should have no appreciable effect on the separation of the peptides. Nevertheless, the retention times and peak capacities were less at pH 3.0 compared to pH 7.0, when the pH effect on separation of the synthetic peptides using monolithic column 8 was investigated using salt gradient elution (data not shown). Peak no. 4 eluted even later than 70 min at pH 7.0. This pH effect on separation of peptides was reported earlier [23,25]. Mant and Hodges [38] explained that the effect was due to a reduction in the column capacity to retain charged species as the pH became more acidic, which is not desirable.

Fig. 6 shows the effects of pH on retention time, peak capacity, and resolution between α-chymotrypsinogen A and cytochrome C using monolithic column 8. With an increase in pH, the retention time of each protein decreased. Ribonuclease A eluted before α-chymotrypsinogen A and cytochrome C when the pH was 8.0 or higher, while it eluted later at pH values of 6.0 and 7.0. This effect can be used to optimize various separations. Peak capacities of 15, 17, 17, and 16 were obtained for proteins at pH 6.0, 7.0, 8.0, and 9.0, respectively. The slight variation in peak capacity from pH 6.0 to 9.0 indicates that the column was stable at different pH values. The resolution between α-chymotrypsinogen A and cytochrome C decreased from 3.8 to 2.0 at pH 6.0 and 9.0, respectively.

**Table 4**
Effect of salt gradient on the separation of peptides.[a]

| Gradient rate | Peak 1 | | Peak 2 | | Peak 3 | | Peak 4 | | Peak 5 | | Resolution[d] | Peak capacity[e] |
|---|---|---|---|---|---|---|---|---|---|---|---|---|
| | $t_R$[b] | $w_d$[c] | $t_R$ | $w_d$ | $t_R$ | $w_d$ | $t_R$ | $w_d$ | $t_R$ | $w_d$ | | |
| 2.5% B/min | 12.6 | 1.46 | 14.8 | 1.52 | 16.0 | 1.67 | 18.1 | 1.72 | 69.3 | 4.02 | 1.48 | 19 |
| 5.0% B/min | 10.5 | 1.45 | 12.7 | 1.47 | 14.1 | 1.68 | 16.9 | 1.69 | 53.1 | 3.80 | 1.50 | 10 |
| 10% B/min | 9.49 | 1.38 | 11.1 | 1.00 | 12.4 | 1.28 | 14.3 | 1.14 | 46.0 | 3.50 | 1.35 | 6 |
| 20% B/min | 8.44 | 0.78 | 9.22 | 0.83 | 10.4 | 0.96 | 12.0 | 1.08 | 40.2 | 3.10 | 0.97 | 4 |

[a] *Conditions*: 10.2 cm × 75 μm i.d. column 8; 100% A to 100% B in 40, 20, 10, and 5 min, followed by 100% B, where A was 5 mmol/L phosphate buffer at pH 3.0 and B was 1 mol/L NaCl in A, 40 μL/min pump flow rate, on column detection at 214 nm.
[b] $t_R$ is retention time in min.
[c] $w_d$ is peak width in min.
[d] Resolution between peaks 1 and 2.
[e] Peak capacity was calculated from gradient time/peak width. Peaks 1–4 represent methionine enkephalin, leucine enkephalin, Val-Tyr-Val, Gly-Tyr, and angiotensin II, respectively.

### 3.7. Separation of peptides and protein digest

Monolithic column 8 was applied to separate peptide mixture H2016 using salt gradient elution (Table 4). The structures and characteristics of these natural peptides were described previously [27]. Five peaks were separated without ACN in the mobile phase. With an increase in gradient rate from 2.5% to 20% B/min, the peak capacity decreased from 19 to 4. Acceptable resolution of methionine enkephalin and leucine enkephalin was obtained. Methionine enkephalin (*Mw* 573) and leucine enkephalin (*Mw* 555) have the same charge and chain length, and similar molecular weights and hydrophobicities. Ionic interaction is less for methionine enkephalin than for leucine enkephalin, due to its greater molecular weight, thus, leading to earlier elution. The resolution between methionine enkephalin and leucine enkephalin reduced from 1.48 to 0.97 when gradient rates changed from 2.5% to 20% B/min, respectively. This monolith provided better resolution of methionine enkephalin and leucine enkephalin than the AMPS-PEGDA monolith [23], but worse than the SPMA-PEGDA [25] and PAHEMA-PEGDA [27] monoliths reported earlier.

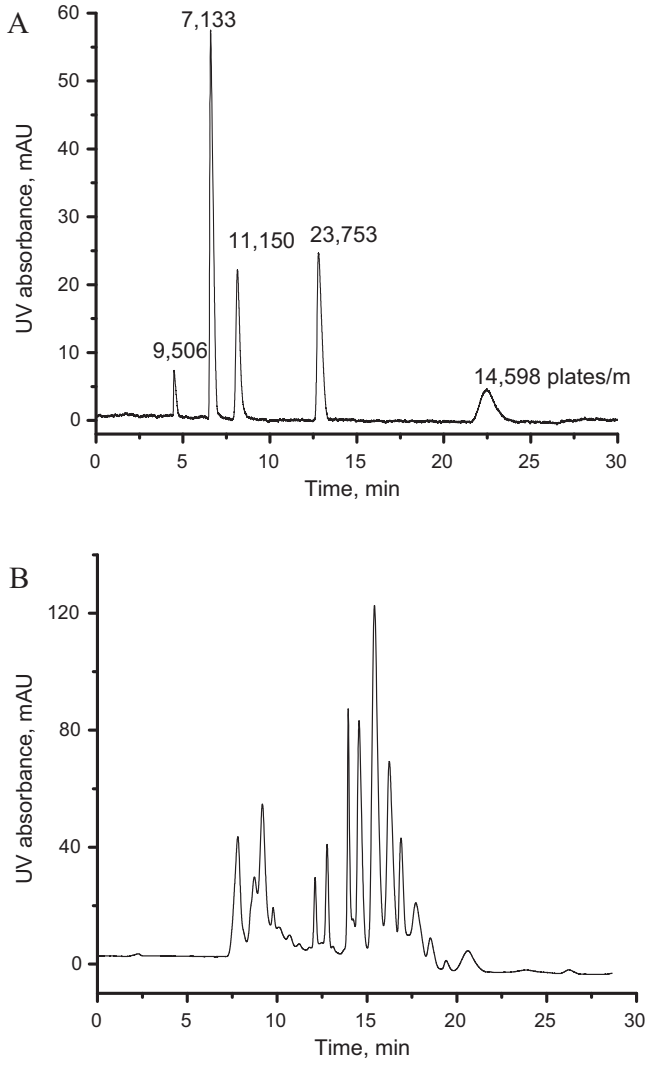


**Fig. 7.** Separation of peptides and cytochrome C digest. Conditions: 14.5 cm × 75 μm i.d. column 8; buffer A was 5 mmol/L phosphate at pH 3.0, buffer B was 1 M NaCl in buffer A; (A) isocratic separation of 100% buffer B; 40 μL/min pump flow rate; (B) linear gradient from 100% buffer A to 100% buffer B in 10 min, followed by 10 min 100% B; 0.2 μL/min pump flow rate; online UV detection at 214 nm. Peak identifications: A: (1) leucine enkephalin, (2) Gly-Tyr, (3) D-Leu-Gly, (4) angiotensin II, and (5) Gly-Gly-Tyr-Arg; B: cytochrome C digest.

Monolithic column 8 was also used to separate a peptide mixture containing D-Leu-Gly, Gly-Gly-Tyr-Arg, Gly-Tyr, angiotensin II, and leucine enkephalin under isocratic elution conditions. With 1 M NaCl in 5 mmol/L sodium phosphate at pH 3.0 as the mobile phase, an efficiency of 13,228 plates/m was achieved (Fig. 7A), which is lower than measured for the CES P0050 peptides, possibly because they are smaller and have different chemical properties.

The column was also used to separate a cytochrome C digest under gradient elution conditions. The separation was carried out in 5 mmol/L sodium phosphate mobile phase with a linear gradient of sodium chloride. The separation is shown in Fig. 7B. Ten major peaks were obtained with some minor peaks.

### 3.8. Reproducibility of the monoliths

The run-to-run and column-to-column reproducibilities were measured using column 8. For three consecutive separations of proteins, interspersed with 20 min equilibrations with 5 mmol/L sodium phosphate at pH 9.0, the RSDs of retention times for the five proteins were 1.37%, 1.52%, 0.457%, 0.935%, and 1.05%. The RSDs of peak widths for the five proteins were 3.09%, 8.27%, 6.18%, 0.830%, and 5.66%. These results indicate good run-to-run reproducibility, confirming the stability of the monolithic material. Column-to-column reproducibility was performed using three columns to separate CES P0050 under isocratic conditions with 20% (v/v) ACN in the mobile phase at pH 3.0. The RSDs of retention times for the four peptides were 3.51%, 2.97%, 2.60%, and 2.03%. The RSDs of peak widths for the four peptides were 16.5%, 14.9%, 9.35%, and 13.3%. The poor RSD values for peak widths most likely arose because we used an on-line detector and manual injection. A slight movement of the column during injection could dramatically affect the peak widths.

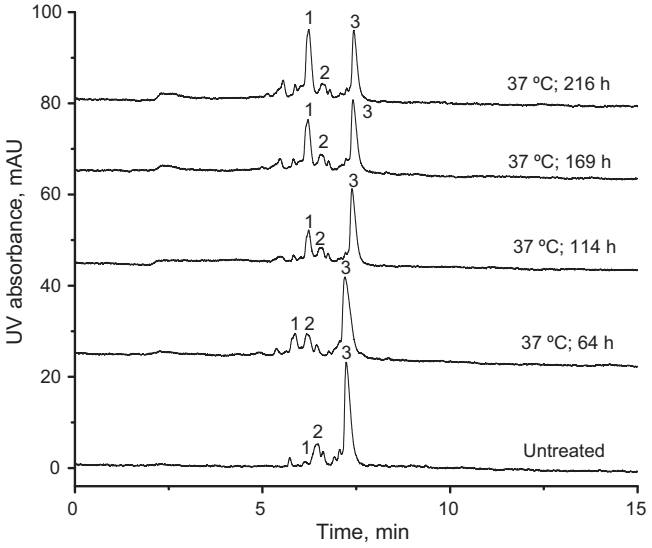


**Fig. 8.** Separation of deamidation variants of ribonuclease A. Conditions: 16.0 cm × 75 μm i.d. column 8; buffer A was 5 mmol/L phosphate at pH 6.0, buffer B was 1 mol/L NaCl in buffer A; linear gradient from 80% buffer B to 90% buffer B in 15 min; 40 μL/min pump flow rate; online UV detection at 214 nm. Peak identifications: (1) and (2) are deamidation products (DP), and (3) is the native ribonuclease A.

### 3.9. Separations of deamidation variants of ribonuclease A

Deamidation of asparagine (Asn) residues is a common structural modification of recombinant protein. It is observed in protein-based pharmaceuticals, including human growth hormone [39], monoclonal antibodies [40], and acidic fibroblast growth factor [41]. It affects the activity or the stability of the therapeutical protein [42]. Hence, monitoring the deamidation variants in proteins is important for quality control in pharmaceutical production. Donato et al. [43] used a cation exchange column, Mono S, followed by hydrophobic interaction chromatography to resolve two deamidation variants and ribonuclease A. It was concluded that the kinetics of deamidation were first order with a half life, $T_{1/2}$, of 178 h. Weitzhandler et al. [42] used a weak cation exchange column, ProPac WCX-10, to separate the two deamidation variants and the native ribonuclease A. Kinetics of first order were observed with a $T_{1/2}$ of 159 h. With monolithic column 8, deamidation variants having Asp and isoAsp at $Asn^{67}$ were separated from each other and from ribonuclease A (Fig. 8). A first order reaction was observed with a $T_{1/2}$ of 195 h. Compared to the $T_{1/2}$ values of 159 and 178 h, the measured 195 h is larger, which might result from the use of an old ribonuclease A sample. Normally, the deamidation rate decreases with incubation time. As can be seen in Fig. 8, an untreated sample already had some deamidation variants. Thus, a large $T_{1/2}$ would be expected.

### 3.10. Characterization and merits of monoliths synthesized from a single monomer

All of the BMEP monoliths were synthesized in 75-μm i.d. fused silica capillaries. Column pressure drops were measured using different solvents (i.e., water, methanol, and ACN) to evaluate the mechanical stabilities, particularly of monolithic column 8. A linear dependence of flow rate on column back pressure was observed, indicating that these monoliths were not compressed at least up to 3 mm/s (back pressure < 2000 psi).

Permeability measurements can be used to study the swelling and shrinking of a monolith. If a monolith swells, its throughpores decrease in size, resulting in lower permeability, and vice versa. The permeability was calculated using Darcy's law, $K = \eta u L/\Delta P$, where $\eta$ is the dynamic viscosity of the mobile phase, $L$ is the column length, $u$ is the linear velocity of the mobile phase, and $\Delta P$ is the column pressure drop. The permeabilities of monolithic column 8 were measured as $9.86 \times 10^{-15}$ m$^2$, $51.3 \times 10^{-15}$ m$^2$, and $20.2 \times 10^{-15}$ m$^2$ for water, methanol, and ACN, respectively. The permeability of the monolith was 5.2 times higher in methanol and 2.0 times higher in ACN than in water. These results indicate that the monolith swelled in aqueous solution. Due to the highly cross-linked structure of the monolith, the swelling may not result from the body of the monolith, but from the ionized functional groups due to the solvent effect. During testing with different solvents, no detachment of the monolith from the capillary wall was observed. The flow rate reached a constant value after equilibration with a new solvent in 3 min, indicating that swelling and shrinking were reversible.

The merits of monoliths synthesized from a single monomer mainly result from (a) high crosslinking which reduces swelling and shrinking, and increases surface area, and (b) makes the optimization of conditions for synthesis easier. Furthermore, with fewer reagents involved in the synthetic method, more reproducible monoliths are expected.

## 4. Conclusions

Cation exchange polymeric monoliths were prepared by *in situ* photo-initiated copolymerization in 75 μm i.d. capillaries using BMEP as a single monomer. The resulting monoliths provided relatively high dynamic binding capacities, and low back pressures. Compared to ion exchange monoliths prepared previously in our laboratory using two monomers [23,25,27], monoliths synthesized from one monomer in this work showed similar DBC values of approximately 50 mg/mL. Lower porosity and permeability were measured due to the more highly cross-linked structures. Good separation of peptides and proteins were obtained with higher resolution. A higher efficiency of approximately 53,000 plates/m was achieved in isocratic separation of peptides and proteins. The monoliths showed negligible hydrophobicity for separations of peptides and proteins.

## References

[1] P.R. Levison, J. Chromatogr. B 790 (2003) 17.
[2] L. Jacob, C. Frech, Biosep. Bioprocess 1 (2007) 127.
[3] C. Mazza, A. Kundu, S.M. Cramer, Biotech. Technol. 12 (1998) 137.
[4] D. Sykora, F. Svec, J.M.J. Fréchet, J. Chromatogr. A 852 (1999) 297.
[5] D.L. Crimmins, R.S. Thoma, D.W. McCourt, B.D. Schwartz, Anal. Biochem. 176 (1989) 255.
[6] F. Wang, J. Dong, X. Jiang, M.Y.H. Zou, Anal. Chem. 79 (2007) 6599.
[7] F. Svec, J. Sep. Sci. 27 (2004) 747.
[8] F. Svec, J. Sep. Sci. 27 (2004) 1419.
[9] E.G. Vlakh, T.B. Tennikova, J. Sep. Sci. 30 (2007) 2801.
[10] M.R. Buchmeiser, Polymer 48 (2007) 2187.
[11] J. Urban, P. Jandera, J. Sep. Sci. 31 (2009) 2521.
[12] E.G. Vlakh, T.B. Tennikova, J. Chromatogr. A 1216 (2009) 2637.
[13] H. Aoki, N. Tanaka, T. Kubo, K. Hosoya, J. Sep. Sci. 32 (2009) 341.
[14] F. Svec, J. Chromatogr. A 1217 (2010) 902.
[15] B. Paull, P.N. Nesterenko, Trends Anal. Chem. 24 (2005) 295.
[16] Z. Liu, R. Wu, H. Zou, Electrophoresis 23 (2002) 3954.
[17] Y. Ueki, T. Umemura, J. Li, T. Odake, K. Tsunoda, Anal. Chem. 76 (2004) 7007.
[18] T. Rohr, E.F. Hilder, J.J. Donovan, F. Svec, J.M.J. Fréchet, Macromolecules 36 (2003) 1677.
[19] C. Viklund, K. Irgum, Macromolecules 33 (2000) 2539.
[20] C. Viklund, F. Svec, J.M.J. Fréchet, J. Biotechnol. Prog. 13 (1997) 597.
[21] A. Palm, M.V. Novotny, Anal. Chem. 69 (1997) 4499.
[22] E.F. Hilder, F. Svec, J.M.J. Fréchet, J. Chromatogr. A 1053 (2004) 101.
[23] B. Gu, Z. Chen, C.D. Thulin, M.L. Lee, Anal. Chem. 78 (2006) 3509.
[24] B. Gu, Y. Li, M.L. Lee, Anal. Chem. 79 (2007) 5848.
[25] X. Chen, H.D. Tolley, M.L. Lee, J. Sep. Sci. 32 (2009) 2565.
[26] J. Krenkova, A. Gargano, N.A. Lacher, J.M. Schneiderheinze, F. Svec, J. Chromatogr. A 1216 (2009) 6824.
[27] X. Chen, H.D. Tolley, M.L. Lee, J. Chromatogr. A 1217 (2010) 3844.
[28] S.H. Lubbad, M.R. Buchmeiser, J. Sep. Sci. 32 (2009) 2521.
[29] A. Greiderer, S.C. Ligon Jr., C.W. Huck, G.K. Bonn, J. Sep. Sci. 32 (2009) 2510.

[30] Y. Li, H.D. Tolley, M.L. Lee, J. Chromatogr. A 1217 (2010) 4934.
[31] J. Vidic, A. Podgornik, A. Štrancar, J. Chromatogr. A 1065 (2005) 51.
[32] http://www.dionex.com/en-us/webdocs/4458-AN125-Cation-Exchange-26Jun09-LPN1045-02.pdf.
[33] C. Viklund, F. Svec, J.M.J. Fréchet, Chem. Mater. 8 (1996) 744.
[34] T.W.L. Burke, C.T. Mant, J.A. Black, R.S. Hodges, J. Chromatogr. 476 (1989) 377.
[35] M. Weitzhandler, D. Farnan, J. Horvath, J.S. Rohrer, R.W. Slingsby, N. Avdalovic, C. Pohl, J. Chromatogr. A 828 (1998) 365.
[36] A. Greiderer, L. Trojer, C.W. Huck, G.K. Bonn, J. Chromatogr. A 1216 (2009) 7747.
[37] S. Bouhallab, G. Henry, E. Boschetti, J. Chromatogr. A 724 (1996) 137.
[38] C.T. Mant, R.S. Hodges, J. Chromatogr. 326 (1985) 349.
[39] A.B. Johnson, J.M. Shirokawa, W.S. Hancock, M.W. Spellman, L.J. Basa, D.W. Aswad, J. Biol. Chem. 624 (1989) 14262.
[40] J. Cacia, C.P. Quan, M. Vasser, M.B. Sliwkowski, J. Frenz, J. Chromatogr. 634 (1993) 229.
[41] D.B. Volkin, A.M. Verticelli, M.W. Bruner, K.E. Marfia, P.K. Tsai, C.R. Middaugh, M.K. Sardana, J. Pharm. Sci. 84 (2006) 7.
[42] M. Weitzhandler, D. Farnan, J.S. Rohrer, N. Avdalovic, Proteomics 1 (2001) 179.
[43] A.D. Donato, M.A. Ciardiello, M.D. Nigris, R. Piccoli, L. Mazzarella, G. D'Alessio, J. Biol. Chem. 268 (1993) 4745.